Electronic Supplementary Information

Enhancing Low-field Magnetoresistance in Magnetite Nanoparticles *via* Zinc Substitution

Tao Wang,[a] Zhong-Zhi Luan,[b] Jing-Yuan Ge,[a] Ling Liu,[d] Di Wu,[b] Zhong-Peng Lv,[*a] Jing-Lin Zuo,[*a] Shouheng Sun[*c]

[a]*State Key Laboratory of Coordination Chemistry, School of Chemistry and Chemical Engineering, Collaborative Innovation Center of Advanced Microstructures, Nanjing University, Nanjing 210093, P. R. China*

[b]*National Laboratory of Solid State Microstructures, Department of Physics, Collaborative Innovation Center of Advanced Microstructures, Nanjing University, Nanjing 210093, P. R. China*

[c]*Department of Chemistry, Brown University, Providence, Rhode Island 02912, USA*

[d]*Institute of Theoretical and Computational Chemistry, Key Laboratory of Mesoscopic Chemistry of the Ministry of Education (MOE), School of Chemistry and Chemical Engineering, Nanjing University, Nanjing, 210093, P. R. China*

[*] Email: zuojl@nju.edu.cn; ssun@brown.edu.

Table S1. ICP-AES data of the TDA-coated $Zn_xFe_{3-x}O_4$ NPs at different Zn^{2+} ion substitution level (x = 0, 0.1, 0.2, 0.3, 0.4 and 1) and the OAm-coated Fe_3O_4 sample obtained from same washing and drying procedure.

Samples	Fe mg/L	Zn mg/L	Zn substitution level (%)	Percentage deviation from the initial ratio of precursors	Mass percentage of $Zn_xFe_{3-x}O_4$	Packing density* ($1/nm^2$)
x = 0 (TDA)	9.31 ±0.02	0	0	0%	85.2% ±0.4%	2.9 ±0.3
x = 0.1 (TDA)	8.76 ±0.02	0.36 ±0.001	10 ±0.04	0%	84.5% ±0.4%	3.1 ±0.3
x = 0.2 (TDA)	8.59 ±0.02	0.59 ±0.001	17 ±0.05	15%	84.9% ±0.3%	3.1 ±0.3
x = 0.3 (TDA)	8.06 ±0.02	0.86 ±0.002	25 ±0.08	16.7%	84.2% ±0.4%	3.2 ±0.4
x = 0.4 (TDA)	8.18 ±0.02	1.26 ±0.003	35 ±0.11	12.5%	86.4% ±0.4%	2.8 ±0.3
x = 1 (TDA)	5.48 ±0.01	3.22 ±0.006	100 ±0.18	0%	88.2% ±0.4%	3.5 ±0.5
x = 0 (OAm)	9.22 ±0.02	0	0	0%	87.1% ±0.4%	2.0 ±0.3

* We assume that all the NPs are spherical and identical with the diameters as shown in Fig. S1 respectively. Surfactants can be considered as brushes anchored to the spheres. The packing density of TDA or OAm is equal to the number of surfactants divided by the global surface area.

Table S2. XRD results for $Zn_xFe_{3-x}O_4$ samples

	2θ of peak (311) (°) [a]	Lattice parameter (Å) [a]	FWHM (°) [a]	Crystal size (nm) [b]	Hard core size obtained from TEM (nm)	Difference between crystal and hard core size (nm) [c]
$x = 0$	35.66 [0.003]	8.362 [0.006]	1.454 [0.006]	6.652 [0.03]	6.93 ±0.58	−0.278 [−4.01%]
$x = 0.1$	35.49 [0.004]	8.385 [0.009]	1.442 [0.008]	6.690 [0.04]	7.17 ±0.61	−0.480 [−6.69%]
$x = 0.2$	35.48 [0.004]	8.392 [0.008]	1.461 [0.008]	6.604 [0.04]	7.32 ±0.64	−0.716 [−9.79%]
$x = 0.3$	35.47 [0.004]	8.402 [0.006]	1.458 [0.008]	6.617 [0.04]	7.11 ±0.68	−0.493 [−6.93%]
$x = 0.4$	35.42 [0.007]	8.408 [0.003]	1.477 [0.010]	6.529 [0.05]	7.29 ±0.68	−0.761 [−10.4%]

[a] The values of standard error in square brackets are obtained from *Jade 6.0* or *Origin*.
[b] The error values in square brackets produced by propagation of error are obtained from Scherrer's formula.
[c] The percentages in square brackets are decreased percentage of crystal sizes compared with hard core sizes.

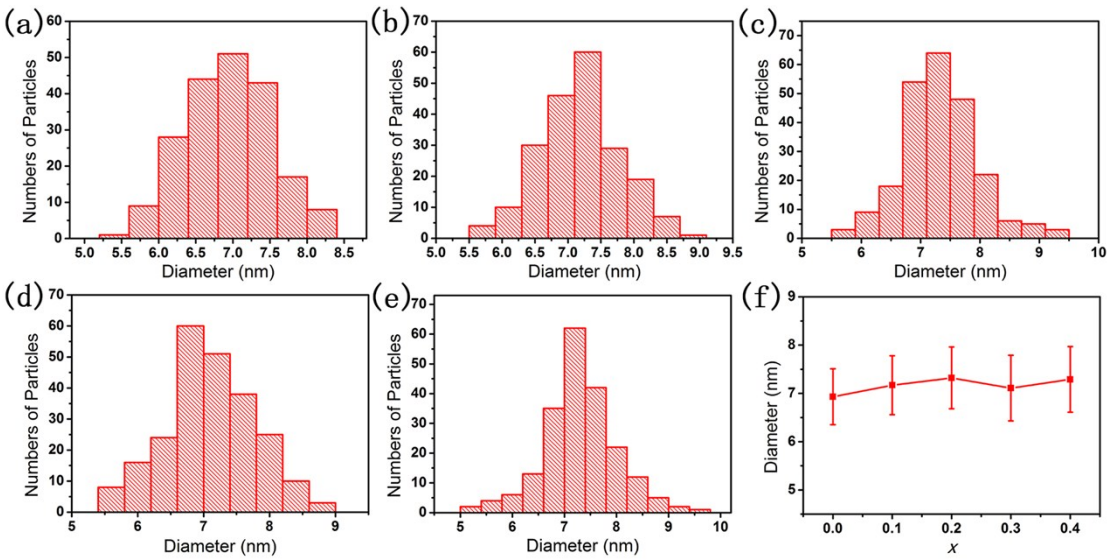

Fig. S1. Size distributions of (a) Fe_3O_4; (b) $Zn_{0.1}Fe_{2.9}O_4$; (c) $Zn_{0.2}Fe_{2.8}O_4$; (d) $Zn_{0.3}Fe_{2.7}O_4$; (e) $Zn_{0.4}Fe_{2.6}O_4$ NP cores obtained from statistical analysis of over 200 particles from TEM images. (f) The means and standard deviations of the particle sizes

for $Zn_xFe_{3-x}O_4$ NPs at different Zn^{2+} substitution level (x = 0, 0.1, 0.2, 0.3 and 0.4).

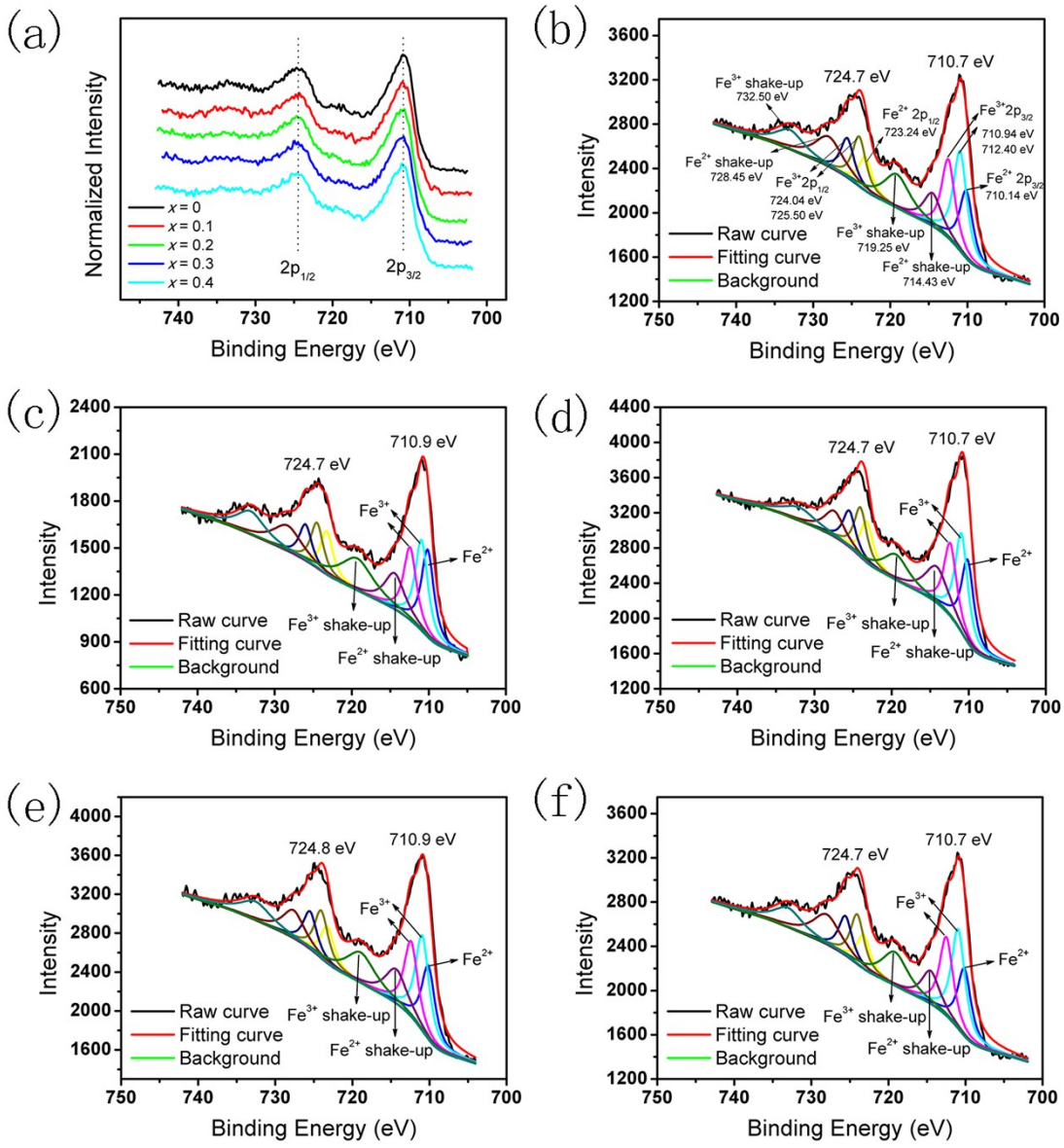

Fig. S2. (a) XPS Fe 2p spectra of $Zn_xFe_{3-x}O_4$ (x = 0, 0.1, 0.2, 0.3 and 0.4) NPs. (b) Deconvolution of Fe 2p peak for the sample of (b) x = 0; (b) x = 0.1; (d) x = 0.2; (e) x = 0.3; (f) x = 0.4. The binding energies of related sub peaks are set as identical in all Fe 2p spectra, and detailed positions of sub peaks are shown in (b).

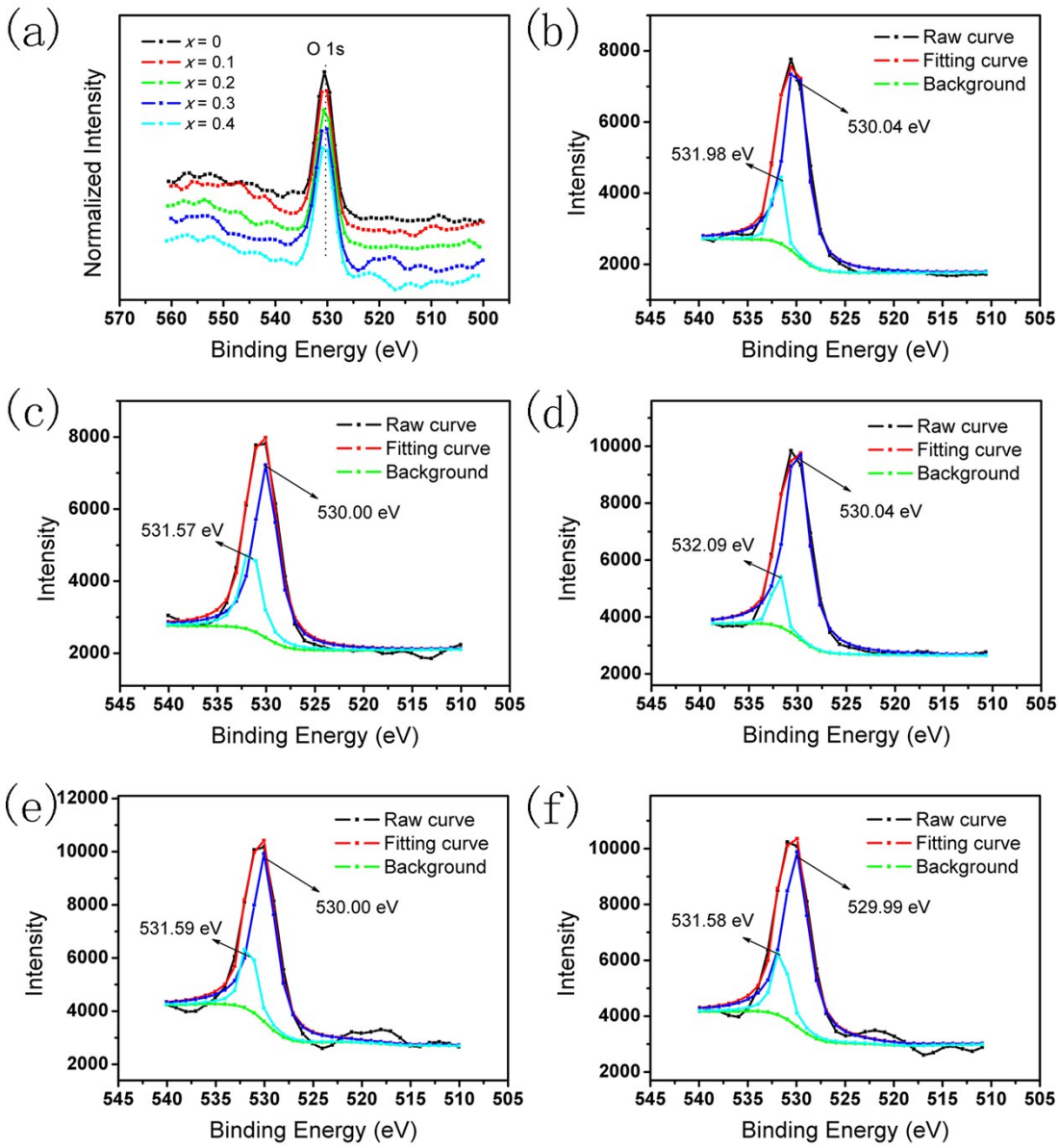

Fig. S3. (a) XPS O 1s spectra of $Zn_xFe_{3-x}O_4$ (x = 0, 0.1, 0.2, 0.3 and 0.4) NPs. (b) Deconvolution of O 1s peak for the sample of (b) x = 0; (b) x = 0.1; (d) x = 0.2; (e) x = 0.3; (f) x = 0.4.

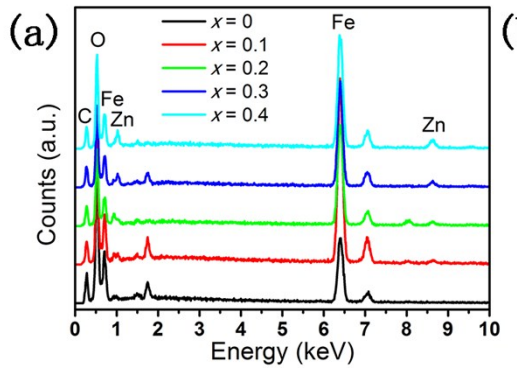

(b)

EDS	Fe Atom%	Zn Atom%	Zn doping level (%)
$x = 0$	100	0	0
$x = 0.1$	96.5±0.4	3.5±0.4	10.4±1
$x = 0.2$	93.4±0.7	6.6±0.7	19.9±2
$x = 0.3$	91.1±0.6	8.9±0.6	26.7±2
$x = 0.4$	88.0±0.9	12.0±0.9	36.0±3
$x = 1$	61.8±0.3	38.2±0.3	114±1

Fig. S4. (a, b) Energy dispersive X-ray spectroscopy (EDS) data of the TDA-coated $Zn_xFe_{3-x}O_4$ NPs at different Zn^{2+} ion substitution level (x = 0, 0.1, 0.2, 0.3, 0.4 and 1).

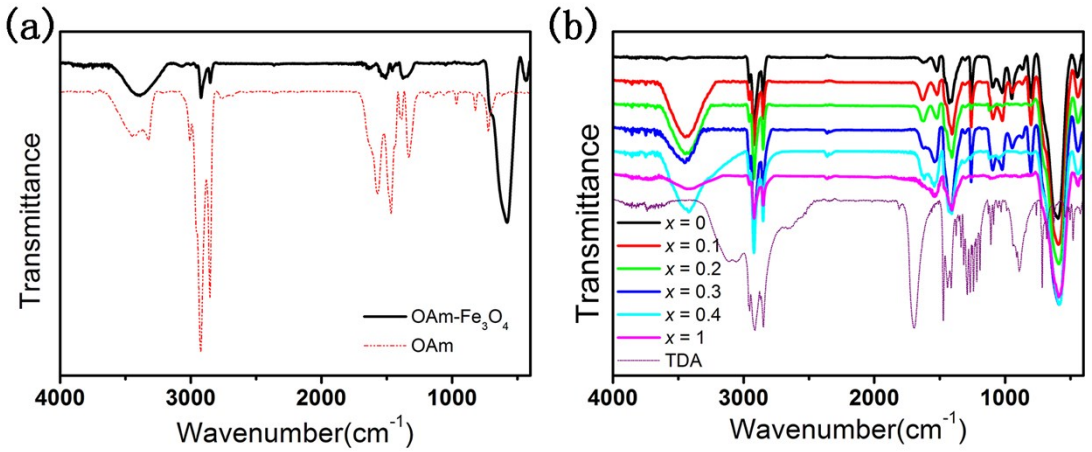

Fig. S5. FT-IR spectra of (a) the OAm-coated Fe_3O_4 NP assembly and OAm, (b) the TDA-coated $Zn_xFe_{3-x}O_4$ NP assemblies and TDA.

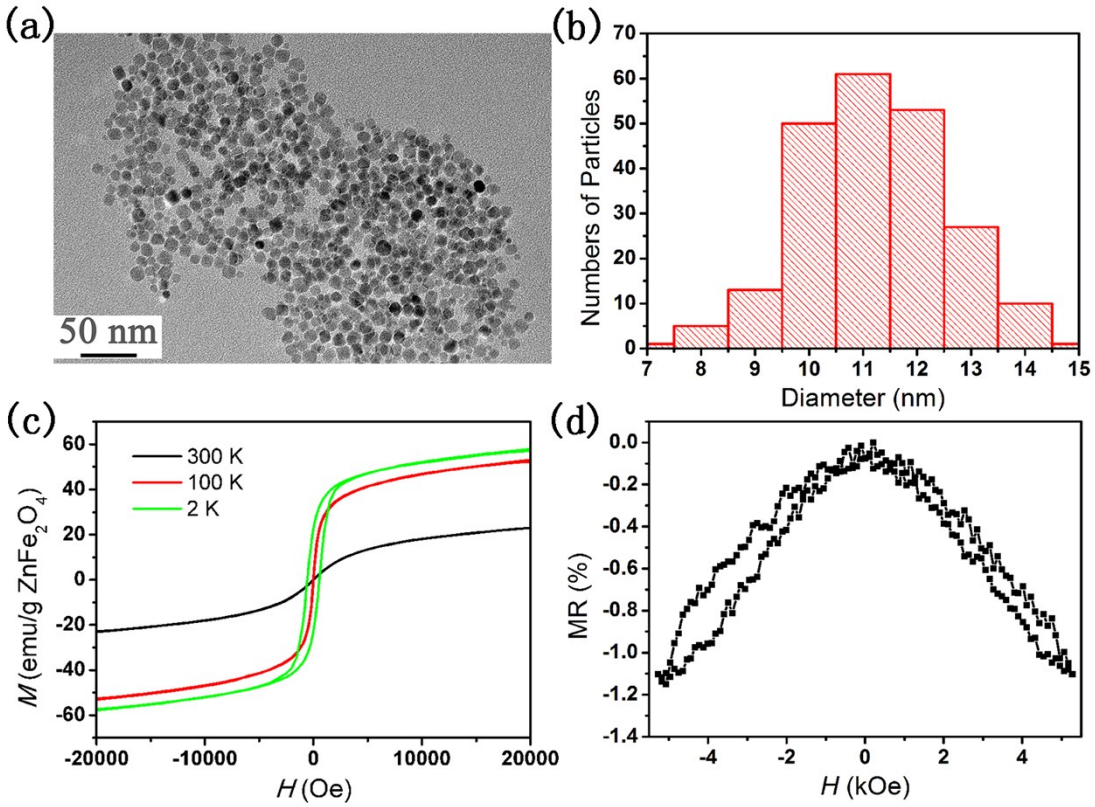

Fig. S6. (a) TEM image of the as-synthesized $ZnFe_2O_4$ nanoparticles, and the scale bar corresponds to 50 nm. (b) Size distributions of $ZnFe_2O_4$ NP cores obtained from statistical analysis of over 200 particles from TEM images. (c) Field-dependent magnetization of the TDA-coated $ZnFe_2O_4$ at 2 K, 100K and 300 K. (d) Magnetic field dependent MR ratio of TDA-coated $ZnFe_2O_4$ NP assembly at 300 K.

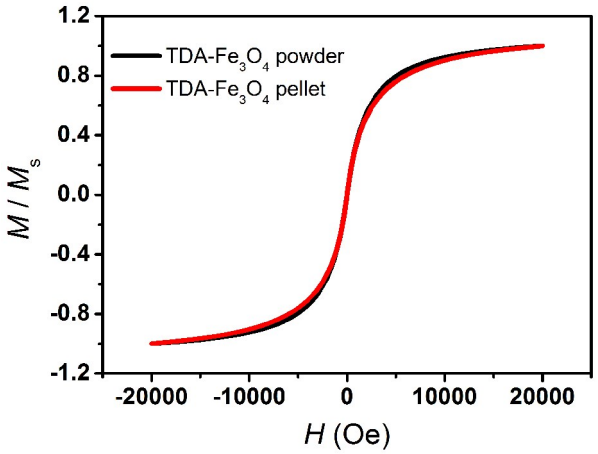

Fig. S7. The comparison between *M*–*H* curves of TDA-Fe_3O_4 before (black curve) and after (red curve) cold-pressing at 300 K.

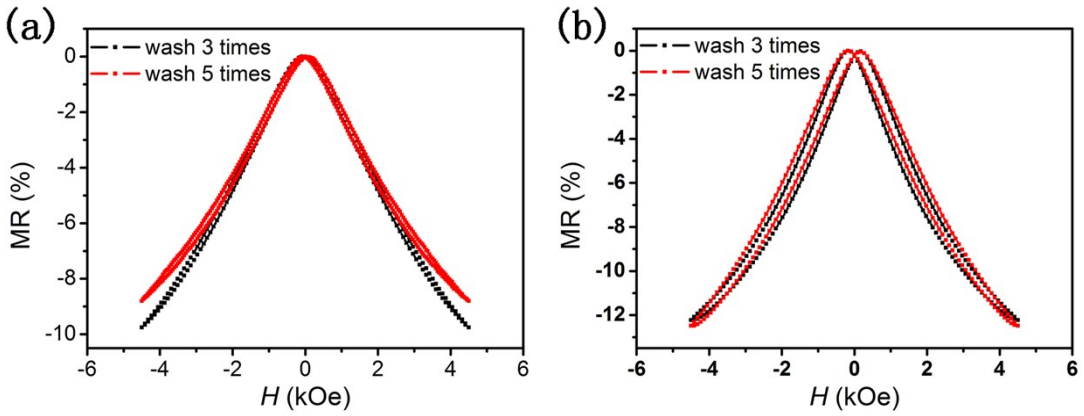

Fig. S8. The comparison of MR ratio of (a) the OAm-coated Fe_3O_4 NP assembly and (b) the TDA-coated $Zn_{0.1}Fe_{2.9}O_4$ NP assembly with different washing cycles at 300 K.

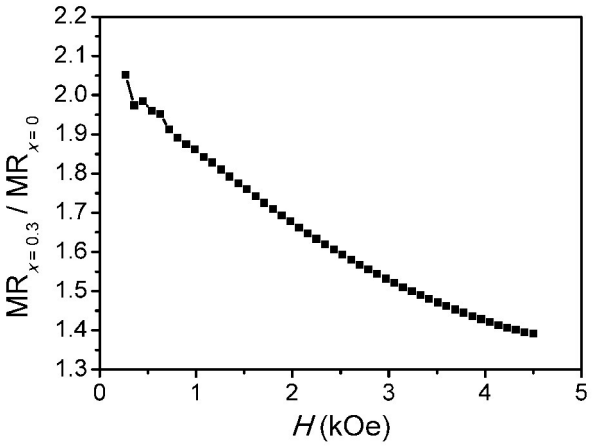

Fig. S9. Field-dependent ratio of MR of TDA-coated $Zn_{0.3}Fe_{2.7}O_4$ to MR of TDA coated Fe_3O_4 at 300 K.